

# Development and Reaction Mechanism Introduction of Cu-Based Catalysts Applied to CO<sub>2</sub>RR

Xichen Feng<sup>a</sup> \*

<sup>a</sup> School of Materials and Chemistry, University of Shanghai for Science & Technology, Shanghai, 200093, China

Corresponding Author: Xichen Feng

---

**Abstract** Since the oil crisis, research on the synthesis of clean and renewable energy has received widespread attention. Electrochemical reduction has proven to be an effective approach for converting CO<sub>2</sub> into industrial chemicals and fuels needed by humans. Cu-based materials, as catalysts capable of converting CO<sub>2</sub> into various carbon products, play a crucial role in the industrialization of CO<sub>2</sub>RR and have achieved remarkable results through the efforts of researchers. However, for true industrial application, Cu-based catalysts still face significant challenges, such as difficulty in achieving high selectivity for specific target products, catalyst reconstruction, and structural instability. In this regard, this paper introduces the mechanism of CO<sub>2</sub>RR and the current development status of Cu-based catalysts, providing insights for future design.

---

Date of Submission: 12-05-2026

Date of Acceptance: 26-05-2026

---

## I. Introduction

Carbon dioxide (CO<sub>2</sub>), as a widely present greenhouse gas, accounts for approximately 0.03% to 0.04% of the total atmospheric volume and plays a role in retaining heat on the ground<sup>1-2</sup>. However, since the Industrial Revolution, the large-scale use of fossil fuels has led to a sharp increase in atmospheric CO<sub>2</sub> levels. According to relevant reports, global CO<sub>2</sub> concentrations have risen from about 280 ppm at the end of the 18th century to 415 ppm in recent years, triggering a series of significant problems: global warming, rising sea levels, loss of biodiversity, acid rain, and more<sup>3</sup>. Moreover, as society develops, human demand for energy continues to rise, and the use of fossil fuels shows no sign of decreasing. Therefore, it is imperative to develop green, recyclable clean energy and to curb and reduce the current atmospheric CO<sub>2</sub> levels. Converting CO<sub>2</sub> into raw materials urgently needed for daily life and industrial production can not only address the issue of excessive CO<sub>2</sub> levels but also reduce the production costs of industrial raw materials. To this end, researchers are attempting to achieve this goal through various technological approaches<sup>2,4</sup>.

Among the various approaches, electrocatalysis can convert CO<sub>2</sub> into a variety of high-value carbon products (such as C<sub>2</sub>H<sub>4</sub>, C<sub>2</sub>H<sub>5</sub>OH, C<sub>3</sub>H<sub>8</sub>O, etc.)<sup>5-7</sup>. Compared to other methods, it offers advantages such as no restrictions on working environment, high energy conversion efficiency, and a wide range of achievable products. Additionally, it enables the effective utilization of wind and solar power, which are often unstable due to their dependence on production conditions and, in most cases, cannot be reliably integrated into the power grid for domestic and industrial use<sup>8</sup>. Electrocatalysis provides an excellent way to harness these renewable energy sources, enabling green production and green usage, thereby playing a significant role in protecting the global environment<sup>9</sup>.

Given the above application demands and the existing research framework, this paper provides a detailed introduction to the reaction mechanism and current development status of electrocatalytic CO<sub>2</sub> reduction technology, with a focus on reviewing the advanced work and recent progress of Cu-based materials in the field of electrocatalytic CO<sub>2</sub> reduction.

### 1. Electrocatalytic CO<sub>2</sub> Reduction Mechanism

Electrocatalytic CO<sub>2</sub> reduction is a complex reaction involving multiple steps and intermediates. Depending on the product, the process involves the transfer of 2, 4, 8, or even more electrons<sup>3</sup>. Table 1 lists the number of electrons transferred and the standard reaction potentials for generating different products during the CO<sub>2</sub>RR process<sup>10-11</sup>. Under conventional conditions, CO<sub>2</sub> molecules are in a chemically inert state<sup>12-13</sup>, which means that breaking the bonds between C and O requires overcoming an energy barrier of approximately 750 kJ·mol<sup>-1</sup>. The thermodynamic and kinetic processes of the reaction play a dominant role in this context.

**Table 1** Potentials required for the formation of reduction products at room temperature, atmospheric pressure,

and pH 7<sup>10-11</sup>.

Reaction Equation	Potential (V vs.RHE)
$\text{CO}_2 + \text{e}^- \rightarrow \text{CO}_2^-$	-0.197
$\text{CO}_2 + 2\text{H}^+ + 2\text{e}^- \rightarrow \text{HCOOH}$	-0.610
$\text{CO}_2 + 2\text{H}_2\text{O} + 2\text{e}^- \rightarrow \text{HCOOH} + \text{OH}^-$	-1.491
$\text{CO}_2 + 2\text{H}^+ + 2\text{e}^- \rightarrow \text{CO} + \text{H}_2\text{O}$	-0.530
$\text{CO}_2 + 2\text{H}_2\text{O} + 2\text{e}^- \rightarrow \text{CO} + 2\text{OH}^-$	-1.347
$2\text{CO}_2 + 2\text{H}^+ + 2\text{e}^- \rightarrow \text{H}_2\text{C}_2\text{O}_4$	-0.913
$2\text{CO}_2 + 2\text{e}^- \rightarrow \text{C}_2\text{O}_4^{2-}$	-1.003
$\text{CO}_2 + 4\text{H}^+ + 4\text{e}^- \rightarrow \text{HCHO} + \text{H}_2\text{O}$	-0.480
$\text{CO}_2 + 3\text{H}_2\text{O} + 4\text{e}^- \rightarrow \text{C} + 4\text{OH}^-$	-1.311
$\text{CO}_2 + 4\text{H}^+ + 4\text{e}^- \rightarrow \text{C} + 2\text{H}_2\text{O}$	-0.200
$\text{CO}_2 + 2\text{H}_2\text{O} + 4\text{e}^- \rightarrow \text{C} + 4\text{OH}^-$	-1.040
$\text{CO}_2 + 6\text{H}^+ + 6\text{e}^- \rightarrow \text{CH}_3\text{OH} + \text{H}_2\text{O}$	-0.380
$\text{CO}_2 + 5\text{H}_2\text{O} + 6\text{e}^- \rightarrow \text{CH}_3\text{OH} + 6\text{OH}^-$	-1.225
$\text{CO}_2 + 8\text{H}^+ + 8\text{e}^- \rightarrow \text{CH}_4 + 2\text{H}_2\text{O}$	-0.240
$\text{CO}_2 + 6\text{H}_2\text{O} + 8\text{e}^- \rightarrow \text{CH}_4 + 8\text{OH}^-$	-1.072
$2\text{CO}_2 + 12\text{H}^+ + 12\text{e}^- \rightarrow \text{CH}_4 + 4\text{H}_2\text{O}$	-0.349
$2\text{CO}_2 + 8\text{H}_2\text{O} + 12\text{e}^- \rightarrow \text{C}_2\text{H}_4 + 12\text{OH}^-$	-1.177
$2\text{CO}_2 + 12\text{H}^+ + 12\text{e}^- \rightarrow \text{C}_2\text{H}_5\text{OH} + 3\text{H}_2\text{O}$	-0.329
$2\text{CO}_2 + 9\text{H}_2\text{O} + 12\text{e}^- \rightarrow \text{C}_2\text{H}_5\text{OH} + 12\text{OH}^-$	-1.157
$2\text{CO}_2 + 14\text{H}^+ + 14\text{e}^- \rightarrow \text{C}_2\text{H}_6 + 4\text{H}_2\text{O}$	-0.270
$3\text{CO}_2 + 18\text{H}^+ + 18\text{e}^- \rightarrow \text{C}_3\text{H}_7\text{OH} + \text{H}_2\text{O}$	-0.310

The thermodynamic theory of E CO<sub>2</sub>RR primarily involves the Gibbs free energy of the reactants and products. As shown by the data listed in Table 1, the activation of CO<sub>2</sub> molecules requires an overpotential of -1.9 V, which exceeds the formation potentials of many reduction products. Therefore, the introduction of catalysts is necessary to lower the energy barrier of the reaction<sup>14</sup>. With the aid of catalysts, CO<sub>2</sub> (activated CO<sub>2</sub>) formed through electron coupling plays an important role in the ECO<sub>2</sub>RR system, as its presence can reduce the overpotential required for product formation. According to the formula  $\Delta G = -nFE$  (where  $\Delta G$  represents Gibbs free energy,  $n$  is the number of electrons transferred,  $F$  is Faraday's constant, and  $E$  is the onset potential), it can be observed that the reaction processes for generating hydrocarbons/alcohols are thermodynamically more favorable compared to CO and HCOOH<sup>15</sup>. However, due to the kinetic barrier imposed by the concentration of mobile protons in the electrolyte, these products are more difficult to obtain in practice. Additionally, as seen in Table 1.1, the potentials required for the formation of all products are lower than the standard potential of HER. Consequently, the competitive hydrogen evolution reaction inevitably occurs during the CO<sub>2</sub>RR process<sup>16</sup>.

The kinetics of E CO<sub>2</sub>RR are directly related to product selectivity and reaction rate. During the CO<sub>2</sub>RR process, CO<sub>2</sub> needs to be converted into final products through the following multiple steps<sup>17-19</sup>: 1) CO<sub>2</sub> molecules dissolve into the electrolyte; 2) CO<sub>2</sub> molecules are transferred from the electrolyte and adsorbed onto the catalyst surface; 3) CO<sub>2</sub> molecules undergo a series of steps to transform into final products; 4) The products desorb from the catalyst surface. Among these, step 3) involves multiple pathways, including C=O bond cleavage, C-C bond coupling, C-H/O-H bond formation, etc., ultimately leading to various carbon-containing products. To date, the CO<sub>2</sub>RR products reported by researchers mainly include the following: 1) C<sub>1</sub> products, including carbon monoxide (CO), formic acid (HCOOH), methane (CH<sub>4</sub>), formaldehyde (HCHO), methanol (CH<sub>3</sub>OH), etc.; 2) C<sub>2</sub> products, including ethylene (C<sub>2</sub>H<sub>4</sub>), ethanol (C<sub>2</sub>H<sub>5</sub>OH), ethane (C<sub>2</sub>H<sub>6</sub>), etc.; 3) C<sub>3+</sub> products, such as propanol (C<sub>3</sub>H<sub>7</sub>OH). Furthermore, improving proton transfer is an effective strategy for optimizing kinetic steps, with noticeable effects achieved by using suitable electrolytes (e.g., carbonates, bicarbonates) and electrolysis cells (e.g., flow cells). Electron transfer is another key point, as it not only controls the final product selectivity but is also closely related to the reaction rate. The electron transfer capability primarily depends on the conductivity of the catalyst and the electrolyte. Selecting highly conductive catalysts/substrates and electrolytes can effectively optimize the electron transfer capability.

The complete reaction pathway of E CO<sub>2</sub>RR involves multiple processes, starting with the activation of CO<sub>2</sub> molecules adsorbed on the catalyst surface (i.e., the formation of CO<sub>2</sub><sup>\*</sup>) and the bending of the linear molecular structure<sup>20-21</sup>. Depending on the binding mode, CO<sub>2</sub><sup>\*</sup> interacts with the catalyst in the forms of <sup>\*</sup>COOH and <sup>\*</sup>OOCH (represents the active site on the catalyst surface). If the active sites of the catalyst bind strongly with the C atom of CO<sub>2</sub><sup>\*</sup>, the <sup>\*</sup>COOH configuration tends to form. Additionally, the binding strength of C-/O-<sup>\*</sup> can be tuned by electron-poor/electron-rich sites on the catalyst surface—due to electrostatic interactions, O tends to bind to electron-poor sites, while C atoms prefer electron-rich sites. As the reaction proceeds, the <sup>\*</sup>OOCH intermediate gains e<sup>-</sup> and H<sup>+</sup> to form HCOOH and desorbs, while <sup>\*</sup>COOH converts to <sup>\*</sup>CO and desorbs as CO. Among these, <sup>\*</sup>CO is a key intermediate capable of generating a series of high-value-added products: For C<sub>1</sub> products, the process involves C–O bond cleavage, C–H and O–H bond formation, along with additional 2e<sup>-</sup>, 4e<sup>-</sup>, and 6e<sup>-</sup> reactions, ultimately yielding HCHO, CH<sub>3</sub>OH, and CH<sub>4</sub>. For C<sub>2</sub> products, the dimerization of <sup>\*</sup>CO, <sup>\*</sup>CHO, and <sup>\*</sup>COH is the rate-determining step, followed by the formation of <sup>\*</sup>COCO, <sup>\*</sup>COCHO, and <sup>\*</sup>COCOH, leading to the final products. For C<sub>3</sub> products, the reaction pathway is similar to that of C<sub>2</sub> products but involves

an additional trimerization step. Based on the above brief description, the CO<sub>2</sub>RR pathways for C<sub>1</sub>, C<sub>2</sub>, and C<sub>3</sub> products are illustrated in Figure 1<sup>22</sup>.

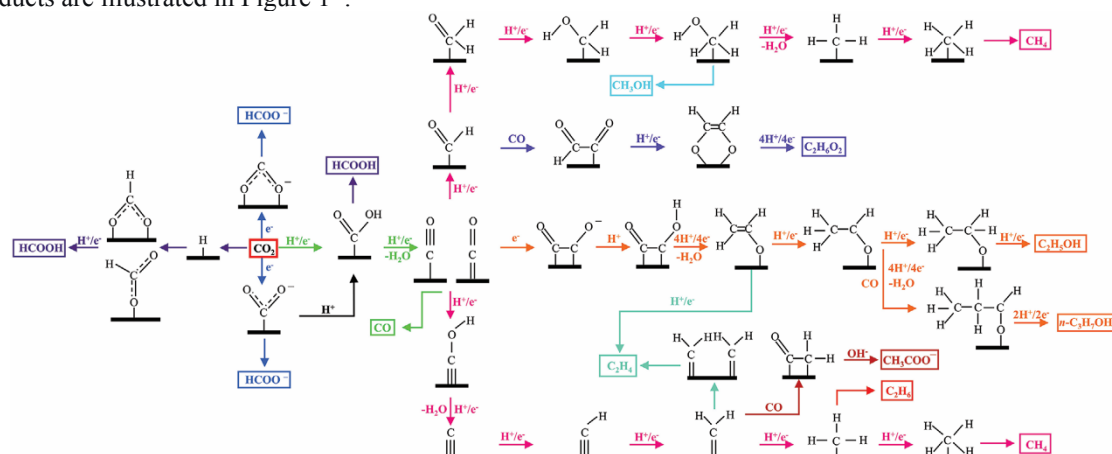


Figure 1. Schematic illustration of the reaction pathways for the formation of various compounds via CO<sub>2</sub>RR<sup>22</sup>.

## 2. Research Progress of Cu-Based Catalysts

Copper-based materials can reduce CO<sub>2</sub> to a variety of products (including C<sub>1</sub> and C<sub>2+</sub>), and their wide selectivity range makes them ideal catalysts for electrocatalytic CO<sub>2</sub> reduction systems. Through continuous research, various different copper-based catalyst systems have been developed. This section provides an overview of the design strategies for CO<sub>2</sub>RR electrocatalysts, including single-metal Cu, Cu alloys, Cu oxides, and Cu compounds.

**Single-metal Cu catalysts:** Single-metal Cu catalysts are the simplest and earliest studied Cu-based catalysts, with preparation methods including wet chemical reduction and electrodeposition<sup>23-24</sup>. The wet chemical reduction method typically uses strong reducing agents such as sodium borohydride (NaBH<sub>4</sub>) or hydrazine hydrate (N<sub>2</sub>H<sub>4</sub>·H<sub>2</sub>O) to reduce copper salts to metallic Cu. The electrochemical deposition strategy, on the other hand, employs a three-electrode working system to reduce and deposit copper species from the electrolyte onto a prepared substrate. By adjusting relevant parameters during the reaction process, such as applied voltage/current, deposition time, solution pH, type of copper salt, and electrolyte concentration, the structure and morphology of the Cu catalyst can be effectively controlled. Therefore, this method is more popular than the wet chemical reduction approach. Chen et al. prepared a Cu<sup>0</sup>-rich catalyst grown on the surface of an Au working electrode using electrochemical deposition<sup>25</sup>. Electrochemical analysis showed that it possesses a significantly enhanced active surface area and reduced charge transfer resistance, while the Faradaic efficiency for C<sub>2</sub>H<sub>4</sub> remained stable above 40%. Tu et al. developed an alkali-ion adsorption-controlled electrodeposition method to grow Cu nanocrystals with controllable morphology<sup>26</sup>. In flow cell reactor tests, the Cu nanocrystals achieved a Faradaic efficiency of over 80% for C<sub>2+</sub> products. In situ attenuated total reflection Fourier-transform infrared spectroscopy and density functional theory calculations confirmed that alkali ions (Li<sup>+</sup>, Na<sup>+</sup>, K<sup>+</sup>, Cs<sup>+</sup>) added to the electrolyte play a regulatory role in the growth of the Cu nanocrystals.

**Cu Alloy Catalysts:** By incorporating additional metals into the system to form Cu-based alloys, the electronic structure of the catalytically active centers can be effectively tuned, thereby altering the adsorption strength of reaction intermediates, enhancing the selectivity for target products, while suppressing the competitive hydrogen evolution reaction. Xie et al. employed density functional theory to calculate the adsorption strength of intermediates on various metal-Cu alloys<sup>27</sup>. Their study showed that under acidic conditions, X-Cu (X = W, Cr, Mo, etc.) type alloys exhibit stronger adsorption for \*CO<sub>2</sub> and \*CO than for \*H, favoring the formation of C<sub>2+</sub> products. Research has indicated that the doping amount of the non-Cu metal in the alloy can influence product distribution. Li et al. prepared Cu-Pd alloys with different atomic ratios using wet chemical reduction and electrochemical replacement strategies<sup>28</sup>. The test results showed that at low Pd content (Cu/Pd-0.25%, Cu/Pd-0.5%), the selectivity for C<sub>2+</sub> products was higher; however, when the Pd content increased (Pd > 1%), the FE<sub>CO</sub> increased by 3-5 times. Using in situ Raman spectroscopy, the authors found that the \*CO on the surface of Cu/Pd-1% mainly consists of low-frequency band \*CO, which is more favorable for the formation of C<sub>2+</sub> products. DFT calculations confirmed that the bimetallic Cu-Pd catalyst enhances the adsorption of \*CO and lowers the energy barrier for C-C coupling. Shang et al. prepared Cu-Sn alloy catalysts (Cu<sub>x</sub>Sn<sub>y</sub>) with different ratios using electrodeposition<sup>29</sup>. Among them, low-entropy Cu<sub>5</sub>Sn achieved a Faradaic efficiency of 64% for ethanol, while high-entropy Cu<sub>6</sub>Sn<sub>5</sub> mainly produced formic acid. This difference is attributed to the enhanced adsorption of key intermediates for ethanol formation on low-entropy Cu<sub>5</sub>Sn. To date, widely reported Cu alloy catalysts include Cu-Ag, Cu-Pd, Cu-Au, Cu-Sn, Cu-Gd, Cu-Mg, Cu-Zn, and Cu-Mo. These introduced atoms generally enhance the adsorption capacity of \*CO on the catalyst surface, making them

suitable for the preparation of C<sub>2+</sub> products. Hoang et al. used DAT as an inhibitor during electrodeposition to prepare high-surface-area Cu-Ag nanowire catalysts (CuAg-wire)<sup>30</sup>. Compared to single-metal Cu-wire, CuAg-wire increased the Faradaic efficiency of C<sub>2</sub>H<sub>4</sub> from less than 40% to nearly 60%, while maintaining an FE<sub>C<sub>2</sub>H<sub>5</sub>OH</sub> of about 25%. Subsequent electrochemical mechanism tests and in situ Raman spectroscopy indicated that the stable Cu oxide overlayer on the catalyst surface, together with Ag, promotes \*CO dimerization, thereby facilitating the conversion to C<sub>2+</sub> products. Furthermore, through structural tuning, Cu-based alloys can also achieve high selectivity for C<sub>2+</sub> products. Ren et al. reported a Cu-Sn alloy (Cu<sub>97</sub>Sn<sub>3</sub>), in which isolated Sn sites exhibited an extremely high surface density (8%). Compared to Cu<sub>100</sub> and Cu<sub>70</sub>Sn<sub>30</sub>, Cu<sub>97</sub>Sn<sub>3</sub> achieved an FE<sub>CO</sub> close to 100%. The authors stated that density functional theory demonstrates that the unique Cu-Sn local coordination environment of Cu<sub>97</sub>Sn<sub>3</sub> plays a crucial role in modulating the types of reaction intermediates.

**Cu Oxides:** Cu oxide (OD-Cu) catalysts, primarily composed of CuO and Cu<sub>2</sub>O, feature characteristics such as multiple grain boundaries, low coordination numbers, and specific oxygen content, demonstrating promising potential for the production of high-value multi-carbon compounds like C<sub>2</sub>H<sub>4</sub>, C<sub>2</sub>H<sub>5</sub>OH, and C<sub>3</sub>H<sub>8</sub>O<sup>12, 31-32</sup>. Extensive research has been conducted on the morphology and grain boundaries of OD-Cu catalysts. Mandal et al. attempted to elucidate the role of grain boundaries by preparing nanoneedles (NNs), nanocubes (NCs), and nanoparticles (NPs)<sup>33</sup>. XRD confirmed the corresponding crystal facets of the catalysts, including the Cu<sub>2</sub>O (111) and (200) facets for NNs, the Cu<sub>2</sub>O (200) facet for NCs, and the Cu<sub>2</sub>O (111) facet for NPs. Theoretical calculations confirmed that after the initiation of the CO<sub>2</sub>RR reaction, the reduction of Cu<sub>2</sub>O to Cu is inevitable, leading to the formation of numerous defects and grain boundaries due to the stripping of oxygen atoms, thereby enhancing catalytic performance. Lei et al. investigated the difference in activity between pristine metallic Cu and Cu generated through in situ reduction during the reaction. They prepared HQ-Cu, containing Cu, CuO, and Cu<sub>2</sub>O, via thermal quenching, as well as AN-Cu through anodization. HAADF-STEM and EELS observations revealed that Cu oxides were reduced to Cu during the reaction, and the reduced HQ-Cu maintained a high Faradaic efficiency for C<sub>2</sub>H<sub>4</sub>, demonstrating that C<sub>2+</sub> product selectivity is not directly related to a specific oxidation state of Cu. Although OD-Cu catalysts exhibit good selectivity for C<sub>2+</sub> products, their unstable oxidation state makes them highly susceptible to reduction and reconstruction during the reaction. To address this, researchers have proposed various stabilization strategies. Jang et al. constructed Al-doped CuO materials (CuO-Al)<sup>34</sup>. SEM observations showed that the addition of Al caused CuO to reconstruct into a nanosheet structure during the reaction while maintaining high selectivity for C<sub>2+</sub> products.

**Cu-Based Compounds:** Compared to single-metal Cu, alloys, and oxides, Cu-based compounds are the most widely reported category of catalysts, covering an extensive range. Based on the position of their anions in the periodic table, they include Group B (primarily B), Group C (primarily C), Group S (S, Se, etc.), and the halogens (F, Cl, Br, etc.)<sup>35-36</sup>.

The electronic configuration of the B atom is 2s<sup>2</sup> 2p<sup>1</sup>, possessing one occupied and five empty p orbitals, which allows it to effectively tune the valence state of Cu<sup>35, 37</sup>. Additionally, the Lewis acid nature of B enables it to accept electrons from Cu, making the local electronic structure of Cu more positive, thereby promoting the conversion of CO<sub>2</sub> to C<sub>2+</sub> products. Sargent et al. reported that B doping can improve the stability of Cu<sup>+</sup> and effectively enhance the production of C<sub>2</sub> products (FE > 80%). Cu atoms located near B exhibit a raised d-band center and positively charged characteristics, which demonstrate stronger binding energy for CO and enhanced CO + CO dimerization.

Carbon (C) materials are widely used in the field of electrocatalysis due to their ability to serve as conductive platforms for active sites and active phases. In recent years, significant progress has been made in the study of CO<sub>2</sub> conversion to tunable carbonaceous products catalyzed by Cu modulated by C materials, mainly focusing on carbon-supported SACs and cluster materials. Similar to C, nitrogen (N) materials, with three unpaired electrons and diverse coordination forms, are particularly notable. N atoms tend to retain lone pair electrons when forming compounds, possess a small atomic radius, short coordination bond lengths, and strong interatomic bonding forces, making them ideal candidates for the development of coordination catalysts. The work by Yin et al. indicated that Cu<sub>3</sub>N nanocubes prepared via a solvothermal method exhibit good CO<sub>2</sub>RR selectivity and stability<sup>38</sup>. Theoretical calculations demonstrated that the exposed Cu<sub>3</sub>N (100) facets can effectively promote CO-CHO coupling, while N vacancies also help stabilize Cu<sup>+</sup>, thereby providing sustained reactivity.

Chalcogen elements, also known as Group O elements, generally refer to O, S, Se, Te, etc. Since Cu oxides have already been discussed separately in the OD-Cu section, the chalcogen elements reviewed in this section do not include O. Chalcogen elements are widely used to construct advanced copper-based catalytic materials due to their versatility and accessibility<sup>39-41</sup>. Among them, metal sulfides possess good electrical conductivity, tunable electronic structures, and flexible compositions, and have been widely applied in the field of catalysis—for example, MoS<sub>2</sub> is an ideal HER material. Copper-based sulfides (Cu<sub>x</sub>S<sub>y</sub>) offer low cost and high abundance. A series of studies have been conducted on the application of sulfur-doped thin films. Research has shown that the presence of S can alter the oxidation state of Cu centers, affecting the adsorption behavior of

key intermediates. Similar to OD-Cu, S in the catalyst is also leached during the CO<sub>2</sub>RR process, facilitating the formation of abundant anion vacancies and active centers with tunable electronic and coordination structures. The outermost electronic configuration of Se is similar to that of S and O, but Se has a larger atomic radius and lower electronegativity, thus exhibiting unique characteristics in modulating the valence state of Cu and the reduction reaction pathway. Se coordination can increase the covalency of metal–anion bonds and the d-orbital occupancy of Cu, because Se has lower electronegativity than O<sup>42</sup>. Catalytically active Cu centers with modulated electron density can promote intermediate CO adsorption, prolong CO residence time, and lead to increased hydrogen adsorption in the vicinity through Lewis acid–base interactions, thereby facilitating the formation of more C<sub>2+</sub> products. Research on tellurium-coordinated copper-based catalysts is relatively limited. Tellurium has low electronegativity and forms more covalent bonds with copper than sulfur and selenium. In chalcogen-modified copper systems, tellurium introduces low-basicity sites with weaker blocking effects on adjacent copper atoms, leading to poor formic acid selectivity. However, precise design can make copper telluride an efficient CO<sub>2</sub>RR catalyst.

Halogen (F, Cl, Br, I) atoms, due to their unique electronic configurations, can readily combine with Cu atoms in catalysts (in the order F < Cl < Br < I)<sup>32,37</sup>. F is typically used to promote electron transfer and charge redistribution in copper-based catalysts, while Cl-, Br-, and I- ions may introduce defects, owing to their different ionic radii (F<sup>-</sup>: 0.136 nm, Cl<sup>-</sup>: 0.181 nm, Br<sup>-</sup>: 0.196 nm, I<sup>-</sup>: 0.220 nm) and decreasing electronegativity (F<sup>-</sup> > Cl<sup>-</sup> > Br<sup>-</sup> > I<sup>-</sup>). Research has shown that the presence of halide ions, either in Cu-based catalysts or in the electrolyte, can influence surface reconstruction during electrochemical oxidation/reduction cycles, providing effective strategies for the development of highly stable copper-based catalysts.

## II. Conclusion

Converting CO<sub>2</sub> into industrial chemicals and fuels needed by humans through electrochemical reduction has been proven to be an effective means of mitigating the greenhouse effect, offering advantages such as high energy efficiency, environmental friendliness, and low cost. Among these, Cu-based catalysts hold great promise due to their ability to convert CO<sub>2</sub> into a variety of C<sub>2+</sub> products. However, although Cu-based compounds provide numerous solutions to meet the demands for various chemical feedstock productions and have achieved some success in practical industrial applications, there are still notable shortcomings that cannot be ignored, such as poor selectivity and insufficient stability. At the same time, the phase and structural changes of the catalysts during the reaction remain poorly understood. Therefore, there is an urgent need to develop low-cost, green electrocatalysts with high product selectivity, good stability, and a well-understood reaction mechanism.

- [1]. Martens, J.; Bogaerts, A.; De Kimpe, N.; Jacobs, P.; Marin, G.; Rabaey, K.; Saeys, M.; Verhelst, S., The Chemical Route to a Carbon Dioxide Neutral World. *Chemsuschem* **2017**, *10* (6), 1039-1055.
- [2]. Service, R., ENERGY Carbon capture marches toward practical use. *Science* **2021**, *371* (6536), 1300-1300.
- [3]. Gong, F.; Zhu, H.; Zhang, Y.; Li, Y., Biological carbon fixation: From natural to synthetic. *Journal Of CO2 Utilization* **2018**, *28*, 221-227.
- [4]. Li, A.; Cao, Q.; Zhou, G.; Schmidt, B.; Zhu, W.; Yuan, X.; Huo, H.; Gong, J.; Antonietti, M., Three-Phase Photocatalysis for the Enhanced Selectivity and Activity of CO<sub>2</sub> Reduction on a Hydrophobic Surface. *Angewandte Chemie-International Edition* **2019**, *58* (41), 14549-14555.
- [5]. Wu, H.; Yu, H.; Chow, Y.; Webley, P.; Zhang, J., Toward Durable CO<sub>2</sub> Electroreduction with Cu-Based Catalysts via Understanding Their Deactivation Modes. *Advanced Materials* **2024**, *36* (31).
- [6]. Harmon, N.; Wang, H., Electrochemical CO<sub>2</sub> Reduction in the Presence of Impurities: Influences and Mitigation Strategies. *Angewandte Chemie-International Edition* **2022**, *61* (12).
- [7]. Zhang, X.; Wang, Z.; Chen, Z.; Zhu, Y.; Liu, Z.; Li, F.; Zhou, W.; Dong, Z.; Fan, J.; Liu, L., Molecular trapdoor mechanism of InSSZ-13(MP) holds promise for selective electrochemical reduction of CO<sub>2</sub> at low concentrations. *Applied Catalysis B-Environment And Energy* **2022**, *317*.
- [8]. Diercks, C.; Liu, Y.; Cordova, K.; Yaghi, O., The role of reticular chemistry in the design of CO<sub>2</sub> reduction catalysts. *Nature Materials* **2018**, *17* (4), 301-307.
- [9]. Wang, C.; Wang, X.; Ren, H.; Zhang, Y.; Zhou, X.; Wang, J.; Guan, Q.; Liu, Y.; Li, W., Combining Fe nanoparticles and pyrrole-type Fe-N<sub>4</sub> sites on less-oxygenated carbon supports for electrochemical CO<sub>2</sub> reduction. *Nature communications* **2023**, *14* (1), 5108.
- [10]. Xu, Y.; Chu, X.; Li, Y.; Jiang, Z.; Yuan, Q.; Sun, K.; Wang, A.; Jiang, J.; Lee, J.; Fan, M., Recent Progress and Challenges of Cu-Based Catalysts in Electrochemical Urea Synthesis with CO<sub>2</sub> and Diverse Waste N Sources. *Small* **2026**, *22* (5).
- [11]. Wang, C.; Sun, Y.; Chen, Y.; Zhang, Y.; Yue, L.; Han, L.; Zhao, L.; Zhu, X.; Zhan, D., In Situ Electropolymerizing Toward EP-CoP/Cu Tandem Catalyst for Enhanced Electrochemical CO<sub>2</sub>-to-Ethylene Conversion. *Advanced Science* **2024**, *11* (34).
- [12]. Liu, X.; Li, L.; Zhao, G.; Xiong, P., Optimization strategies for CO<sub>2</sub> biological fixation. *Biotechnology Advances* **2024**, *73*.
- [13]. Duan, Y.; Ruan, W.; Guan, J., Optimization strategies for carbon dioxide electroreduction to ethylene. *Chemical Engineering Journal* **2025**, *510*.
- [14]. Birdja, Y.; Pérez-Gallent, E.; Figueiredo, M.; Göttle, A.; Calle-Vallejo, F.; Koper, M., Advances and challenges in understanding the electrocatalytic conversion of carbon dioxide to fuels. *Nature Energy* **2019**, *4* (9), 732-745.
- [15]. Yao, L.; Ding, J.; Cai, X.; Liu, L.; Singh, N.; Mccrory, C.; Liu, B., Unlocking the Potential for Methanol Synthesis via Electrochemical CO<sub>2</sub> Reduction Using CoPc-Based Molecular Catalysts. *ACS Nano* **2024**, *18* (33), 21623-21632.
- [16]. Yin, J.; Jin, J.; Yin, Z.; Zhu, L.; Du, X.; Peng, Y.; Xi, P.; Yan, C.; Sun, S., The built-in electric field across FeN/Fe<sub>3</sub>N interface for efficient electrochemical reduction of CO<sub>2</sub> to CO. *Nature Communications* **2023**, *14* (1).

- [17]. Kim, K.; Kim, W.; Lim, H.; Lee, E.; Kim, H., Tuned Chemical Bonding Ability of Au at Grain Boundaries for Enhanced Electrochemical CO<sub>2</sub> Reduction. *Acs Catalysis* **2016**, *6* (7), 4443-4448.
- [18]. He, Q.; Lee, J.; Liu, D.; Liu, Y.; Lin, Z.; Xie, Z.; Hwang, S.; Kattel, S.; Song, L.; Chen, J., Accelerating CO<sub>2</sub> Electroreduction to CO Over Pd Single-Atom Catalyst. *Advanced Functional Materials* **2020**, *30* (17).
- [19]. Zhang, B.; Ren, L.; Xu, Z.; Cheng, N.; Lai, W.; Zhang, L.; Hao, W.; Chu, S.; Wang, Y.; Du, Y.; Jiang, L.; Liu, H.; Dou, S., Atomic Structural Evolution of Single-Layer Pt Clusters as Efficient Electrocatalysts. *Small* **2021**, *17* (26).
- [20]. Maulana, M.; Lee, H.; Gyan-Barimah, C.; Sung, J.; Yu, J., Hollow PtCo alloy nanostructures for efficient oxygen reduction electrocatalysis in polymer electrolyte membrane fuel cells. *Journal Of Materials Chemistry A* **2024**, *12* (41), 27979-27986.
- [21]. Wiranarongkorn, K.; Eamsiri, K.; Chen, Y.; Arpornwichanop, A., A comprehensive review of electrochemical reduction of CO<sub>2</sub> to methanol: Technical and design aspects. *Journal Of CO<sub>2</sub> Utilization* **2023**, *71*.
- [22]. Guo, Y.; Li, Y.; Wang, X.; Wang, L.; Wang, Z., Recent advances in electrochemical C-N coupling for carbon and nitrogen emissions reduction and resource recovery. *Chemical Engineering Journal* **2024**, *499*.
- [23]. Li, D.; Liu, J.; Chen, X.; Feng, Z.; Wang, S.; Wang, Y.; Lin, N.; Wu, J.; Feng, Y., Regulation of coordinated nitrogen species for atomically dispersed Fe-N<sub>x</sub> catalyst to boost electrocatalytic CO<sub>2</sub>-to-CO conversion. *Applied Catalysis B-Environment And Energy* **2025**, *365*.
- [24]. Zhane, M.; Li, K.; Yuan, S.; Lv, R.; Huang, H.; Hu, H.; Liu, J.; Liu, L.; Fan, M.; Li, K., Mechanism of efficient electroreduction of CO<sub>2</sub> to CO at Ag electrode in imidazolium-based ionic liquids/acetonitrile solution. *Applied Catalysis B-Environment And Energy* **2024**, *359*.
- [25]. Chen, B.; Jiang, Y.; Xiao, H.; Li, J., Selective CO<sub>2</sub>-to-HCOOH Electroreduction on Graphdiyne-Supported Bimetallic Single-Cluster Catalysts. *Acs Catalysis* **2024**, *14* (14), 10510-10518.
- [26]. Tu, W.; Tsai, T.; Tsai, D.; Xie, Y.; Liu, H.; Tsai, M.; Chou, T.; Pan, Y., Cation- and CO<sub>2</sub>-assisted electrochemical synthesis of clean, shape-controlled Cu nanocrystals for selective CO<sub>2</sub> reduction to C<sub>2+</sub> products. *Journal Of Materials Chemistry A* **2025**, *13* (40), 34827-34835.
- [27]. Xie, Y.; Ou, P.; Wang, X.; Xu, Z.; Li, Y.; Wang, Z.; Huang, J.; Wicks, J.; McCallum, C.; Wang, N.; Wang, Y.; Chen, T.; Lo, B.; Sinton, D.; Yu, J.; Wang, Y.; Sargent, E., High carbon utilization in CO<sub>2</sub> reduction to multi-carbon products in acidic media. *Nature Catalysis* **2022**, *5* (6), 564-570.
- [28]. Li, C.; Guo, R.; Zhang, Z.; Wu, T.; Pan, W., Converting CO<sub>2</sub> into Value-Added Products by Cu<sub>2</sub>O-Based Catalysts: From Photocatalysis, Electrocatalysis to Photoelectrocatalysis. *Small* **2023**, *19* (19).
- [29]. Shang, L.; Lv, X.; Zhong, L.; Li, S.; Zheng, G., Efficient CO<sub>2</sub> Electroreduction to Ethanol by Cu<sub>3</sub>Sn Catalyst. *Small Methods* **2022**, *6* (2).
- [30]. Hoang, T.; Verma, S.; Ma, S.; Fister, T.; Timoshenko, J.; Frenkel, A.; Kenis, P.; Gewirth, A., Nanoporous Copper Silver Alloys by Additive-Controlled Electrodeposition for the Selective Electroreduction of CO<sub>2</sub> to Ethylene and Ethanol. *Journal Of The American Chemical Society* **2018**, *140* (17), 5791-5797.
- [31]. Li, J.; Cai, R.; Mu, H.; Guo, J.; Zhong, X.; Wang, J.; Du, X.; Zhang, J.; Li, F., Twin Heterostructure Engineering and Facet Effect Boosts Efficient Reduction CO<sub>2</sub>-to-Ethanol at Low Potential on Cu<sub>2</sub>O@Cu<sub>2</sub>S Catalysts. *Acs Catalysis* **2024**, *14* (5), 3266-3277.
- [32]. Lei, Q.; Zhu, H.; Song, K.; Wei, N.; Liu, L.; Zhang, D.; Yin, J.; Dong, X.; Yao, K.; Wang, N.; Li, X.; Davaasuren, B.; Wang, J.; Han, Y., Investigating the Origin of Enhanced C<sub>2+</sub> Selectivity in Oxide/Hydroxide-Derived Copper Electrodes during CO<sub>2</sub> Electroreduction. *Journal Of The American Chemical Society* **2020**, *142* (9), 4213-4222.
- [33]. Mandal, L.; Yang, K. R.; Motapothula, M. R.; Ren, D.; Lobaccaro, P.; Patra, A.; Sherburne, M.; Batista, V. S.; Yeo, B. S.; Ager, J. W.; Martin, J.; Venkatesan, T., Investigating the Role of Copper Oxide in Electrochemical CO<sub>2</sub> Reduction in Real Time. *Acs applied materials & interfaces* **2018**, *10* (10), 8574-8584.
- [34]. Jang, J.; Lee, K.; Shin, H.; Lee, H.; Lee, B.; Jeong, J.; Kim, J.; Hwang, W.; Park, S.; Bootharaju, M.; Back, S.; Shim, J.; Kim, J.; Hyeon, T.; Sung, Y., Distinct reconstruction of aluminum-doped oxide-derived copper enhances the selectivity of C<sub>2+</sub> products in CO<sub>2</sub> electroreduction. *Journal Of Materials Chemistry A* **2023**, *11* (35), 19066-19073.
- [35]. Fu, J.; Zhu, W.; Chen, Y.; Yin, Z.; Li, Y.; Liu, J.; Zhang, H.; Zhu, J.; Sun, S., Bipyridine-Assisted Assembly of Au Nanoparticles on Cu Nanowires To Enhance the Electrochemical Reduction of CO<sub>2</sub>. *Angewandte Chemie-International Edition* **2019**, *58* (40), 14100-14103.
- [36]. Du, J.; Zhang, G.; Ma, X.; Chang, Q.; Gao, H.; Wang, C.; Du, X.; Li, S.; Wang, T.; Zhao, Z.; Zhang, P.; Gong, J., Electrochemical CO<sub>2</sub> Reduction to Ethanol on Zn-Coordinated Cu Sites Formed by Atmosphere-Induced Surface Reconstruction. *Advanced Functional Materials* **2024**, *34* (51).
- [37]. Chen, T.; Tamilalagan, E.; Govindharaj, A.; Manimaran, P.; Chen, S., Integrating metal oxide-metal hybrids (Cu(II)O-Cu(0)) via electrodeposition for efficient electrochemical reduction of carbon dioxide to valuable carbon products. *Molecular Catalysis* **2026**, *596*.
- [38]. Yin, Z.; Yu, C.; Zhao, Z.; Guo, X.; Shen, M.; Li, N.; Muzzio, M.; Li, J.; Liu, H.; Lin, H.; Yin, J.; Lu, G.; Su, D.; Sun, S., Cu<sub>3</sub>N Nanocubes for Selective Electrochemical Reduction of CO<sub>2</sub> to Ethylene. *Nano Letters* **2019**, *19* (12), 8658-8663.
- [39]. Garcia-Muelas, R.; Dattila, F.; Shinagawa, T.; Martín, A.; Pérez-Ramírez, J.; López, N., Origin of the Selective Electroreduction of Carbon Dioxide to Formate by Chalcogen Modified Copper. *Journal Of Physical Chemistry Letters* **2018**, *9* (24), 7153-7159.
- [40]. Deng, B.; Huang, M.; Li, K.; Zhao, X.; Geng, Q.; Chen, S.; Xie, H.; Dong, X.; Wang, H.; Dong, F., The Crystal Plane is not the Key Factor for CO<sub>2</sub>-to-Methane Electrosynthesis on Reconstructed Cu<sub>2</sub>O Microparticles. *Angewandte Chemie-International Edition* **2022**, *61* (7).
- [41]. Liu, H.; Yang, C.; Bian, T.; Yu, H.; Zhou, Y.; Zhang, Y., Bottom-up Growth of Convex Sphere with Adjustable Cu(0)/Cu(I) Interfaces for Effective C<sub>2</sub> Production from CO<sub>2</sub> Electroreduction. *Angewandte Chemie-International Edition* **2024**, *63* (28).
- [42]. Saxena, A.; Liyanage, W.; Masud, J.; Kapila, S.; Nath, M., Selective electroreduction of CO<sub>2</sub> to carbon-rich products with a simple binary copper selenide electrocatalyst. *Journal Of Materials Chemistry A* **2021**, *9* (11), 7150-7161.